

STUDIES ON THE SIZE AND SHAPE OF CLAY PARTICLES IN AQUEOUS SUSPENSION¹

by

ALLAN KAHN

Shell Development Company, Houston, Texas

ABSTRACT

The size and shape of clay particles in aqueous suspension have been determined by means of five experimental techniques—electro-optical birefringence, ultracentrifugation, viscometry, optical transmission and electron microscopy. Five clay minerals—montmorillonite, illite, hectorite, nontronite and attapulgite—each subdivided into five size fractions, were studied. The average particle dimensions in each fraction are tabulated.

An evaluation of the experimental techniques is presented. It is concluded that for a preliminary survey of the particle size and shape of clay minerals the technique of electron microscopy is best. However, once a model for the particles is obtained, a combination of the techniques of electro-optical birefringence and viscometry becomes more useful in characterizing the size and shape of the particles in suspension.

1. INTRODUCTION

In connection with our fundamental research on clays, a study of the mechanism of flocculation of clay suspensions by electrolytes was considered to be important. To carry out this study it was necessary to develop methods for determining the size and shape of clay particles. However, the size and shape of clay particles are also of intrinsic interest, for these dimensions are among the most important factors in determining the colloidal behavior of clay suspensions.

Most of the available information on clay particle size has come from the direct technique of observation with an electron microscope. However, electron microscopy of clay particles was considered to have several defects. First, the electron micrographs of montmorillonite in the literature, and also some electron micrographs of montmorillonite prepared especially for us, were not clear and were difficult to interpret. Second, in order to obtain the micrograph, the sample must be dried, and hence one cannot be sure that the particles seen in the micrograph correspond to those in suspension. Third, the thickness of the particle cannot be determined from ordinary micrographs, and even with shadowing techniques thicknesses are difficult to determine. Fourth, in projected flocculation studies where an electrolyte is present in addition to the clay, drying of the sample continuously changes the concentration of the electrolyte and thus the flocculation conditions.

¹ Publication no. 147, Shell Development Company, Exploration and Production Research Division, Houston, Texas.

It was therefore decided that other techniques for the determination of size and shape should be investigated. Some work has been done previously (van Olphen, 1950) on the problem of particle size and shape, where the combined techniques of ultramicroscopic counting and viscometry were used. The techniques finally used in our work and the parameters measured are listed below.

<i>Technique</i>	<i>Parameter</i>
(a) Electro-optical birefringence	Maximum length of particle
(b) Ultracentrifugation	Equivalent spherical radius of particle
(c) Viscometry	Ratio of thickness to length of particle
(d) Optical transmission	Maximum length of particle

To characterize particle size fully, the results from two appropriate techniques must be combined. We have used for our calculations the combinations, electro-optical birefringence and ultracentrifugation, and electro-optical birefringence and viscometry.

Electron micrographs¹ of the samples used are also presented in this paper.

2. PREPARATION OF CLAY SAMPLES

Five types of clay—montmorillonite, hectorite, nontronite, illite and attapulgite—were used in our research. The montmorillonite, hectorite and nontronite are examples of the expanding 2:1 lattice-type clay mineral (Marshall, 1949, pp. 51–54). Illite is of the nonexpanding 2:1 lattice type and attapulgite is of the fibrous type.

The sources of the clays used were

(a) Montmorillonite	From Clay Spur, Wyoming
(b) Nontronite	API Sample 33b
(c) Hectorite	API Sample 34a
(d) Illite	API Sample 35
(e) Attapulgite	API Sample 43

A. Preparation of Clay Suspensions

The clays, other than illite, were suspended by slowly dusting the clay into distilled water that was being stirred vigorously. The illite was put into suspension by first digesting the clay in water for 12 hr and then diluting with distilled water. A considerable amount of carbonaceous matter was removed by passing the illite suspension through a very fine screen to remove coarse matter and then treating the suspension with hydrogen peroxide. All the clay suspensions were adjusted to a concentration of 1 percent.

These dilute suspensions were allowed to settle for a few days. Most of the clay "settled out" because of the flocculating effect of the soluble salts in the clay. The clear supernatant liquid was removed and the clays were

¹ Prepared by Dr. T. F. Bates of The Pennsylvania State University.

resuspended in distilled water to the original concentration. This procedure was repeated until the soluble salts had been for the most part removed. The resulting clay suspensions were then washed in the Sharples supercentrifuge several times.

B. Preparation of Suspensions in Sodium Form

The clay suspensions were passed through a cation-exchange resin (Dowex-50) which had been converted to the sodium form by passing an excess of 1 N NaCl through the resin column and then washing the column with distilled water so that the resin bed would be free of all electrolyte. After each pass of the clay through the resin column, the resin was regenerated. The total exchange capacity of the resin was much greater than that of any of the batches of clay suspension used, and several passes of the clay through the resin bed were sufficient to obtain the clay almost completely in the sodium form.

After converting the clay to the sodium form, the suspension was concentrated and resuspended in conductivity water. The final concentrations varied from 1 to 4 percent. The purity of each clay sample was checked by means of x-ray diffraction, and all samples were considered to be satisfactory.

C. Fractionation of Clay Suspensions

To obtain samples of fairly homogeneous particle size, fractionation of each clay sample was made by means of the Spinco ultracentrifuge.

The fractions were obtained by the following treatment: The sample was first centrifuged at 5000 rev./min. for 5 min. The sediment R_1 was collected and the supernatant fluid was then centrifuged at 6000 rev./min. for 10 min. The sediment R_2 from this treatment was collected and the supernatant fluid was centrifuged again. This treatment was continued until five fractions were obtained. The conditions of centrifugation for each of the fractions obtained were

Fraction R_1 —5000 rev./min. for 5 min
 Fraction R_2 —6000 rev./min. for 10 min
 Fraction R_3 —10,000 rev./min. for 15 min
 Fraction R_4 —15,000 rev./min. for 20 min
 Fraction R_5 —20,000 rev./min. for 120 min

On the basis of data presented by the Specialized Instruments Corporation in their service manual, the ranges of the equivalent spherical radius for each fraction were calculated. These size ranges are presented in Table I along with the percentage of each fraction of the various clay minerals.

The actual limits of equivalent spherical radius are not as sharp as delineated. The number given as the lower limit is actually the radius of the smallest particle which, starting at the top layer of liquid, will be centrifuged out under the specified conditions. However, particles of smaller equivalent spherical radius will sediment out also, if they are close enough to the bottom of the centrifuge tube. This factor could be overcome by continually re-

TABLE 1.—DISTRIBUTION BY WEIGHT OF THE CLAY MINERAL FRACTIONS

Fraction	Equivalent Radius, <i>A</i>	Percent by Weight				
		Montmorillonite	Illite	Nontronite	Hectorite	Attapulgitite
<i>R</i> ₁	>1380	27.3	57.8	21.2	53.0	23.6
<i>R</i> ₂	810–1380	15.4	19.4	23.7	9.9	27.1
<i>R</i> ₃	400–810	17.0	12.2	32.6	14.7	36.3
<i>R</i> ₄	230–400	17.9	6.5	15.6	13.8	9.8
<i>R</i> ₅	70–230	22.4	2.7	6.9	4.3	2.0
Residue	<70	—	1.4	—	4.3	1.2

suspending and centrifuging a given fraction, but this was not done with our samples. However, the differences in measured properties between successive fractions in our samples were sufficiently marked for these fractions to be adequate for our purposes.

3. ELECTRO-OPTICAL BIREFRINGENCE STUDIES

The details of the apparatus and theory for the electro-optical birefringence study of clay suspensions have been presented by Kahn and Lewis (1954).

When an electric field is applied to a clay suspension, the clay suspension which is originally isotropic becomes birefringent. This birefringence is attributed to the orientation of particles in the electric field causing a change in the optical properties of the suspension.

The birefringence is measured in the following way: Light that is plane-polarized at 45° to the electric field enters the suspension. When the field is on, the suspension acts as a uniaxial crystal so that the emergent light is elliptically polarized. On passing a quarter-wave plate, the light becomes plane-polarized again but the plane of polarization is rotated through an angle which is directly proportional to the birefringence of the suspension. The light from the quarter-wave plate goes through an analyzer which is "crossed" with the initial plane of polarization of the light. The intensity of light that passes this analyzer is determined by the rotation of the plane of polarization of the light and is thus a measure of the birefringence of the suspension. The intensity of light is measured by means of a photomultiplier tube connected to a cathode-ray oscilloscope.

In our apparatus a rectangular voltage pulse of very short duration is applied to a clay suspension. This pulse and the resulting birefringence curve are shown simultaneously on a dual-channel oscilloscope. At the end of the pulse, the voltage decays rapidly to zero, but the birefringence decays much more slowly. The rate of decay of the birefringence (Benoit, 1951) is given by

$$\frac{\Delta n}{\Delta n_0} = e^{-\delta Dt}, \tag{1}$$

where Δn_0 = initial value of birefringence

Δn = birefringence at time t

D = rotational diffusion constant.

This is generally written in the form

$$\log \Delta n = \log \Delta n_0 - \frac{6}{2.303} Dt. \quad (2)$$

The rotational diffusion constant, which is the desired quantity, may thus be obtained from the slope of a plot of $\log \Delta n$ against t .

The rotational diffusion constant D is related to the size of the particles in the following way (Alexander and Johnson, 1949):
for oblate spheroids (disks)

$$D = \frac{3}{32} \frac{kT}{\eta a^3}, \quad (3)$$

for prolate spheroids (rods)

$$D = \frac{3}{16} \frac{kT}{\pi \eta a^3} \left[4.6 \log \frac{2a}{b} - 1 \right], \quad (4)$$

where k = Boltzmann's constant

T = absolute temperature

η = viscosity of solvent

a = major semi-axis of spheroid

b = minor semi-axis of spheroid.

From previous studies (Marshall, 1949, p. 67) the shape of montmorillonite and illite can best be approximated by disks, and that of attapulgite by rods. Nontronite and hectorite are both lath-shaped. However we shall assume that the major dimension of these particles is that obtained from the formula for oblate spheroids (disks). As the values of a for long rods, and for disks with the same value of D , differ only by a factor of approximately 2.5, the calculated major dimensions for nontronite and hectorite will at least give the proper order of magnitude.

The marked effect of particle size on the birefringence decay curve is shown in Figs. 1 and 2, which are respectively for samples R_1 and R_5 of montmorillonite. In Fig. 1, the decay curve GH of the largest size montmorillonite fraction R_1 is shown. At H , 274 msec after the field has been removed, the sample still has 62 percent of the birefringence at G . In Fig. 2, taken with the smallest montmorillonite fraction R_5 in the cell, 62 percent of the initial birefringence has been reached after the field has been off for only 4 msec. In Fig. 3, the time scale for the R_5 fraction has been expanded so that the decay curve may be obtained more precisely. The discontinuities in the oscilloscope traces of Fig. 3 are caused by the timing signals, which are given every 2 msec.

From an analysis of birefringence curves, such as those shown in Figs. 1 to 3, and the application of equations (2), (3) and (4), the lengths of the major

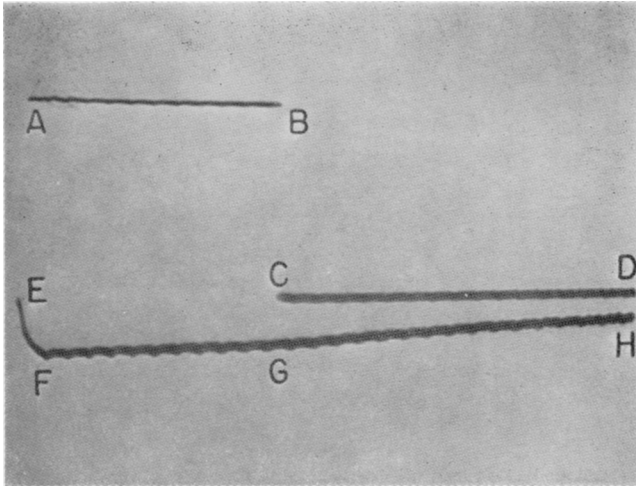


FIGURE 1.—Birefringence curve of sample R_1 . Voltage pulse— $ABCD$: birefringence curve— $EFGH$. Distance AB corresponds to 192.5 msec.

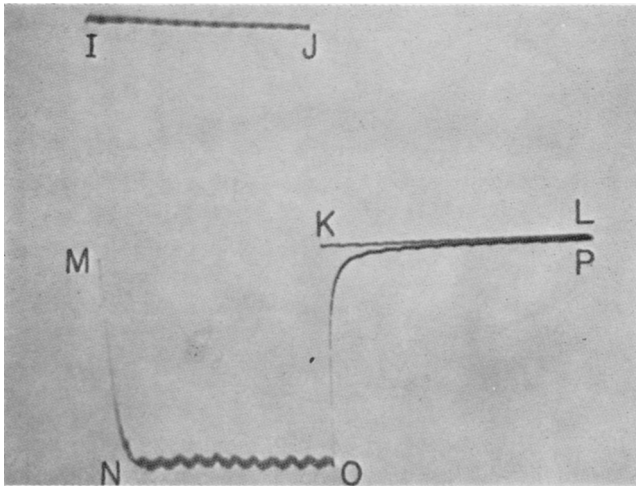


FIGURE 2.—Birefringence curve of sample R_3 . Voltage pulse— $IJKL$: birefringence curve— $MNOP$. Distance IJ corresponds to 192.5 msec.

(To face p. 224)

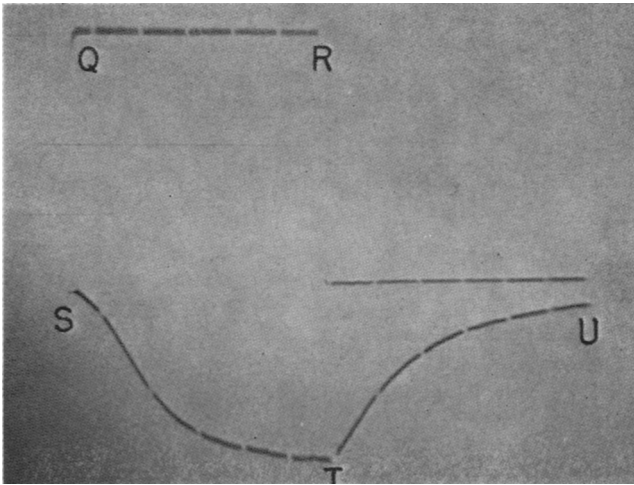


FIGURE 3.—Birefringence curve of sample R_5 . Distance QR corresponds to 10.3 msec.

semi-axes of the clay mineral fractions were calculated. The results are presented in Table 2.

TABLE 2.—LENGTHS OF MAJOR SEMI-AXES OF CLAY MINERAL FRACTIONS

Fraction	Major Semi-axis, A				
	Montmorillonite	Illite	Nontronite	Hectorite	Attapulgite
R_1	12,300	3700	5800	5100–8850	9400–16,400
R_2	10,300	2600	5650	4150–4600	9400–16,100
R_3	3800	2100	4950	3900	7900–14,500
R_4	2950	1900	3750	3350	6650–11,500
R_5	2450	1800	2300	2950	6650

These results will be discussed in section 8 of this report.

4. ULTRACENTRIFUGE STUDIES

A. Theory

The general theory of sedimentation in the ultracentrifuge is well known (Svedberg and Pedersen, 1940). In general when a steady state has been reached in the ultracentrifuge, the centrifugal force equals the frictional force. For spherical particles,

$$\frac{4}{3} \pi r^3 (\rho - \rho_0) \omega^2 x = 6\pi\eta r \frac{dx}{dt}$$

- where r = radius of the particle
- ρ = density of the particle
- ρ_0 = density of solvent
- ω = angular velocity
- x = distance of particle from center of rotation
- η = viscosity of solvent
- t = time

An equivalent calculation can be made if the particle is assumed to be an oblate spheroid of major semi-axis a and minor semi-axis b . The centrifugal force on the particle is $(4/3) \pi a^2 b (\rho - \rho_0) \omega^2 x$. The frictional force on the particle is $(6\pi\eta a F) (dx/dt)$, where F is a "hydrodynamic factor" which is a function of (a/b) . F has been evaluated by Kelley and Shaw (1942), and the results have been checked by us. F approaches fairly rapidly an asymptotic value of 0.66. This value may be used with an error of less than 5 percent for ellipsoids with axis ratios of 10 : 1 or greater.

We have, therefore,

$$\frac{4}{3} \pi a^2 b (\rho - \rho_0) \omega^2 x = 6 \pi \eta \alpha F \frac{dx}{dt}$$

$$(ab)^{\frac{1}{2}} = \left[\frac{9}{2} \frac{dx}{dt} \cdot \eta \right]^{\frac{1}{2}} \cdot F^{\frac{1}{2}}.$$

The quantity in brackets is the expression for the equivalent spherical radius of the particles. Therefore,

$$(ab)^{\frac{1}{2}} = r F^{\frac{1}{2}}$$

and

$$b = \frac{r^2 \cdot F}{a}.$$

Thus, if the major semi-axis of the particle is known from birefringence measurements, the minor semi-axis may be calculated from ultracentrifuge data. In principle, the size and shape of ellipsoidal particles are thus completely determinable.

B. Practical Difficulties

The ultracentrifuge data used in our calculations were obtained with a modified Fisher-Stern apparatus.¹ There are a number of difficulties in the interpretation of these data on clay suspensions which indicate that even under the best of conditions such data probably are not quantitatively reliable.

Theoretically, in the light-absorption method of determining sedimentation boundaries, one expects a "nonsharp" boundary because of diffusion. With clay particles there is the additional complication that particles of exactly the same size will sediment at different rates if their initial orientations are different. Furthermore, in clays the decrease in intensity of the light striking the photographic film, which is used to record the progress of sedimentation, is caused not by absorption but by light scattering. As there is a range of particle sizes in the sample and the scattering is an unknown function of particle size, interpretation of the density of blackening on the photographic plate becomes impossible.

To obtain useful data, one must work at concentrations of about 0.50 percent at which concentration interparticle forces cannot be neglected. The magnitude of the electroviscous effect is uncertain, as is the magnitude of the hydration of the particles, which alters the effective density of the particles.

However, in spite of these many uncertainties, it is estimated that the determination of the equivalent spherical radius in our apparatus should be

¹ The data listed in Table I, obtained with the Spinco ultracentrifuge, were not used in these calculations because of the inherently low precision obtainable with that apparatus, which was designed primarily for preparative work.

reliable within a factor of two or three. In addition, for comparative studies, many of the difficulties enumerated become unimportant.

TABLE 3.—EXPERIMENTAL VALUES OF EQUIVALENT SPHERICAL RADIUS OF SELECTED CLAY FRACTIONS AND CALCULATED VALUES OF MINOR SEMI-AXIS¹

Clay Mineral	<i>R</i> ₁			<i>R</i> ₂			<i>R</i> ₄		
	<i>r</i>	<i>a</i>	<i>b</i>	<i>r</i>	<i>a</i>	<i>b</i>	<i>r</i>	<i>a</i>	<i>b</i>
Montmorillonite	770	12,300	32	535	10,300	18	—	—	—
Nontronite	210	5800	5	—	—	—	130	3750	3
Illite	680	3700	82	—	—	—	240	1900	20

¹ Values of *a*, *b* and *r* are in ångström units.

The values of the equivalent spherical radius obtained for some selected clay fractions are presented in Table 3. In addition, from the equation

$$b = \frac{r^2 F}{a}$$

the values of *b* were calculated for montmorillonite, illite and nontronite on the assumption that the particles were oblate spheroids, using the values of *a* given in Table 2.

These results will be discussed in Section 8.

5. VISCOSITY STUDIES

From viscosity studies, information may be obtained about the asymmetry of particles in suspension. The first theoretical derivation of the viscosity of suspensions was obtained by Einstein. He showed that for a suspension of spheres

$$\eta_r = 1 + 2.5 \phi$$

where η_r = relative viscosity

ϕ = volume fraction of particles.

The derivation for shapes other than spheres is more difficult. Mark and Tobolsky (1950, p. 286) have tabulated the results for rods and disks, taking into account the possible effects of Brownian motion. From their tabulation, it is obvious that the ratio of the axes is the only factor that is related to the relative viscosity. This fact prompted our viscosity investigations.

A. Experimental Method and Results

All viscosities were determined in ASTM size 50 Ostwald viscometers at a temperature of 30.25 ± 0.05°C.

The values of the relative viscosity of suspensions of 0.05 percent concentration¹ of the various clay mineral fractions are presented in Table 4.

TABLE 4.—VALUES OF η_r AND K FOR CLAY MINERAL FRACTIONS

Clay Mineral	R_1		R_2		R_3		R_4		R_5	
	η_r	K	η_r	K	η_r	K	η_r	K	η_r	K
Montmorillonite	1.0260	140	1.0360	194	1.0423	228	1.0427	231	1.0417	225
Nontronite	1.0250	152	1.0362	219	1.0465	282	1.0506	306	1.0440	267
Illite	1.0015	8.5	1.0022	12.5	1.0036	20.4	1.0019	9.8	1.0077	43.7
Hectorite	1.0060	36	1.0095	57	1.0254	153	1.0362	218	1.0325	186
Attapulgitite	1.0076	22.7	1.0122	43.4	1.0140	49.8	1.0166	59.1	1.0109	38.8

If one writes

$$\eta_r = 1 + K \phi$$

as an extension of the Einstein equation, one may calculate K from the experimental values of η_r and ϕ . Such values of K are also listed in Table 4. The value of ϕ was based on the weight concentration of the clay and the density of the clay. However, clay particles have a certain amount of water associated with them in suspension, and this will affect the value of ϕ (and thus of K). A method of evaluating ϕ for any value of the hydration of the clay particle has been given by van Olphen (1951). In our calculations the hydration of the clay particle was not considered, since the error involved in not considering it is considerably less than the uncertainty of the interpretation of the experimental results.

B. Interpretation of Viscosity Results

The mean velocity gradient in an ASTM size 50 viscosity tube is 1350 sec⁻¹. According to the criterion given by Alexander and Johnson (1949, pp. 362-367) if (velocity gradient/rotational diffusion constant) $\gg 1$, the particles are almost completely oriented. Our measurements were made under such circumstances. According to Simha (personal communication), it is plausible that the value for K ,

$$K = \frac{4}{3} \frac{(a/b)}{\tan^{-1}(a/b)}$$

proposed by Jeffery (in Mark and Tobolsky, 1950, p. 286) as a maximum for the viscosity of a suspension of rigid disks without Brownian motion, is the proper one to apply. If in addition it is assumed that a/b is large, so that $\tan^{-1}(a/b) \approx (\pi/2)$, we obtain finally

$$\frac{a}{b} = 1.2 K.$$

¹ Based on weight of clay dried at 105°C.

In combination with the results of electro-optical birefringence, one again may calculate *b*, the minor semi-axis of the particles. The values are given in Table 5.

TABLE 5.—VALUES OF MINOR SEMI-AXIS OF CLAY MINERAL FRACTIONS CALCULATED FROM BIREFRINGENCE AND VISCOSITY DATA¹

Clay Mineral	<i>R</i> ₁ ²			<i>R</i> ₂			<i>R</i> ₃			<i>R</i> ₄			<i>R</i> ₅		
	<i>a</i>	<i>K</i>	<i>b</i>	<i>a</i>	<i>K</i>	<i>b</i>	<i>a</i>	<i>K</i>	<i>b</i>	<i>a</i>	<i>K</i>	<i>b</i>	<i>a</i>	<i>K</i>	<i>b</i>
Montmorillonite	12,300	140	73	10,300	194	44	3800	228	14	2950	231	11	2450	225	9
Nontronite	5800	152	32	5650	219	22	4950	282	15	3750	306	10	2300	267	7
Illite	3700	8.5	360	2600	12.5	173	2100	20.4	86	1900	9.8	162	1800	43.7	34
Hectorite	5100	36	118	4150	57	61	3900	153	21	3350	218	13	2950	186	13
	to	to	to	to	to	to									
	8850	205	4600			67									

¹ Attapulgite data are not included, as the assumed model of the clay particle is invalid for attapulgite.
² Values of *a* and *b* are in ångström units.

6. LIGHT-TRANSMISSION STUDIES

The technique of light scattering is used widely for the determination of particle size and molecular weight in the colloidal range (Bender, 1952). Doty and Steiner (1950) show how the equivalent information may be derived from measurements of optical transmission at various wavelengths.

Doty and Steiner obtain the relation

$$-\frac{d \log \tau}{d \log \lambda} = 4 - \beta, \tag{5}$$

where τ = optical density of suspension

λ = wavelength of light

β = a parameter which is a function only of

d = major dimension of particle

λ_0 = wavelength of light in solution.

In general β increases as d/λ_0 increases. In Figs. 4 to 8, plots of equation (5) are presented for all the clay minerals used in our work. The slopes of the curves were taken at the arbitrarily chosen value of $\tau = 0.1$. In general, the slope increases (or β decreases) with decreasing particle size in agreement with the theory. However, it is not expected that this will be useful in a quantitative way, but it is expected to be qualitatively useful in the ordering of particle sizes for a given kind of clay.

7. ELECTRON MICROSCOPY STUDIES

Electron micrographs were obtained for each of our samples. Representative electron micrographs are presented in Figs. 9 to 13. From each micrograph, the longest dimension was measured for ten particles chosen at random, and an average "major semi-axis" was then calculated for each of the samples. The results are given in Table 6.

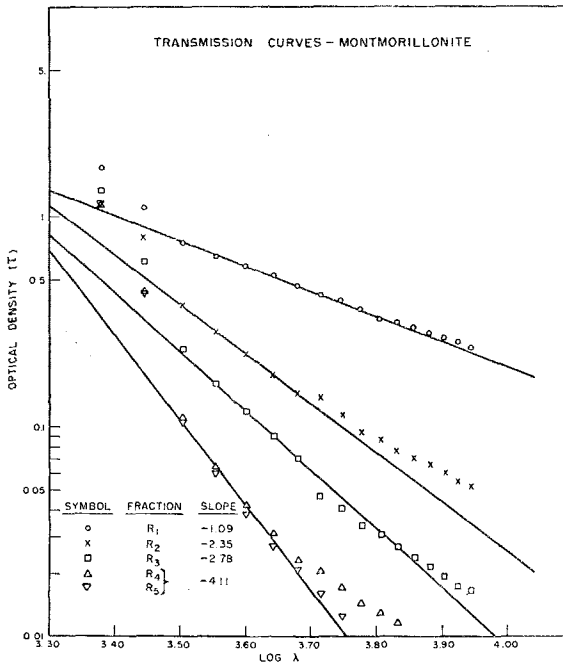


FIGURE 4.—Transmission curves for montmorillonite.

TABLE 6.—LENGTHS OF MAJOR SEMI-AXES OF CLAY PARTICLES FROM ELECTRON MICROSCOPY

Sample	Fraction ¹				
	<i>R</i> ₁	<i>R</i> ₂	<i>R</i> ₃	<i>R</i> ₄	<i>R</i> ₅
Montmorillonite	6900	5400	3380	1620	1350
Nontronite	19,300	8600	7000	5000	3410
Hectorite	5150	3050	3050	3245	2705
Illite	2370	1535	1005	635	535
Attapulgit	7750	6450	5400	4390	3245

¹ Values of *R* in ångström units.

8. DISCUSSION

A. Discussion of Results

1. *Major dimension of particles.*—The major dimension for the particles in each clay fraction was determined by two methods, electro-optical birefringence and electron microscopy. The results are presented in Table 7.

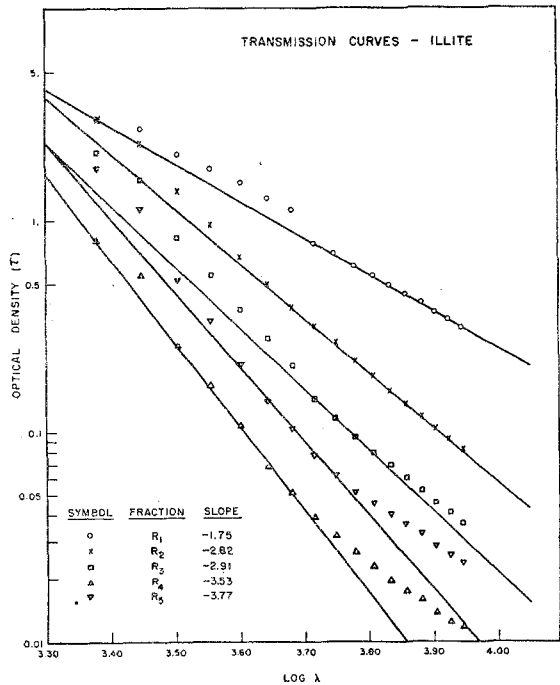


FIGURE 5.—Transmission curves for illite.

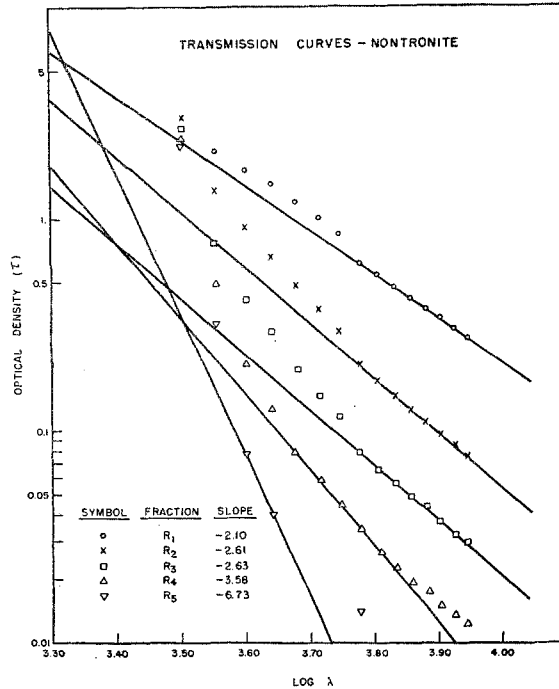


FIGURE 6.—Transmission curves for nontronite.

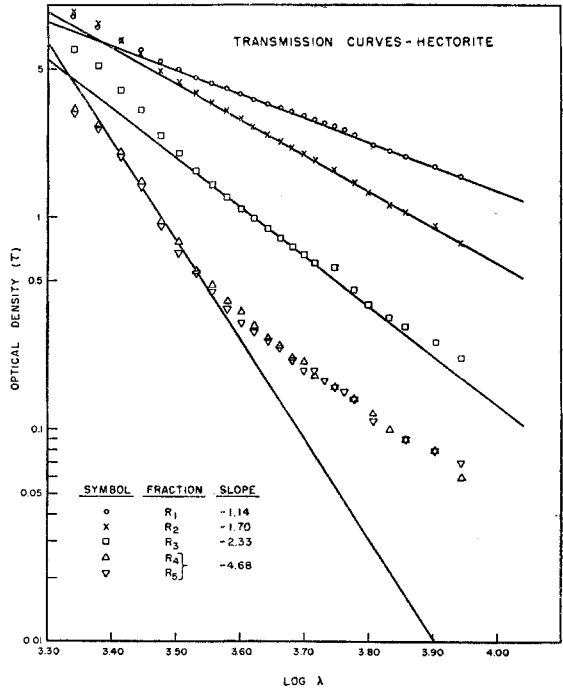


FIGURE 7.—Transmission curves for hectorite.

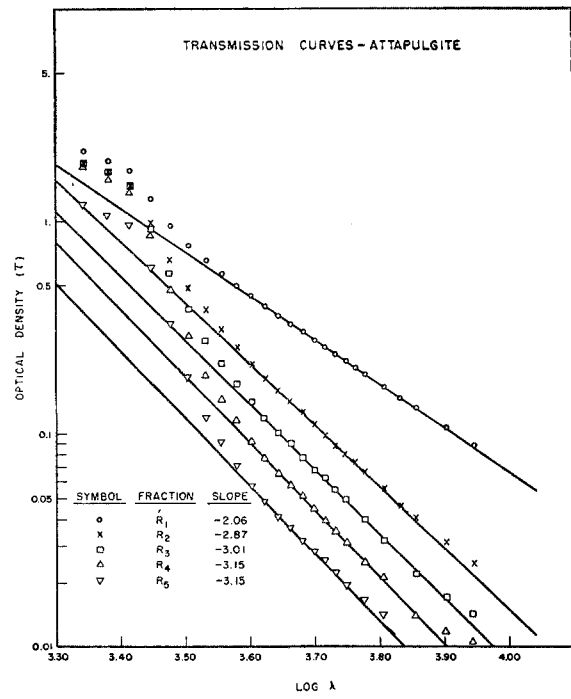


FIGURE 8.—Transmission curves for attapulgite.

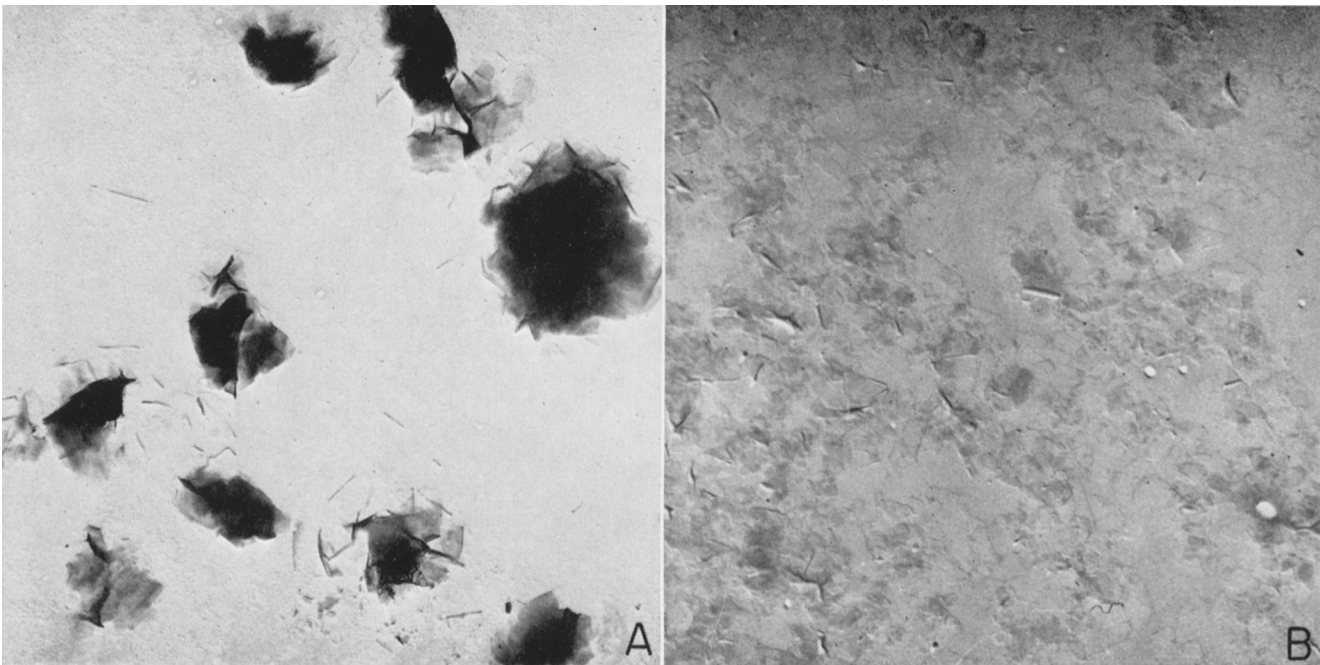


FIGURE 9.—Electron micrographs of montmorillonite ; shadowed with platinum at 10° . A, R_1 , magnification $11,600 \times$. B, R_5 , magnification $14,800 \times$.

(To face p. 232)

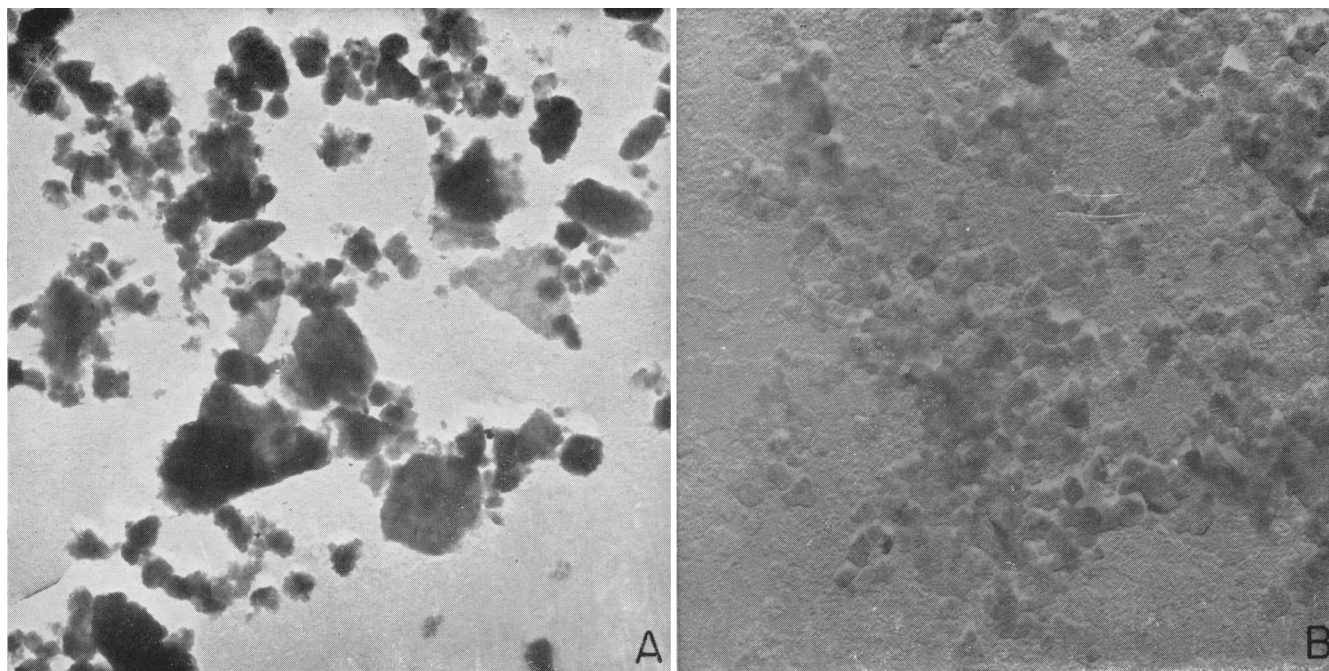


FIGURE 10.—Electron micrographs of illite ; shadowed with uranium at 15° A, R_1 , magnification 11,600 \times . B, R_8 , magnification 28,000 \times .

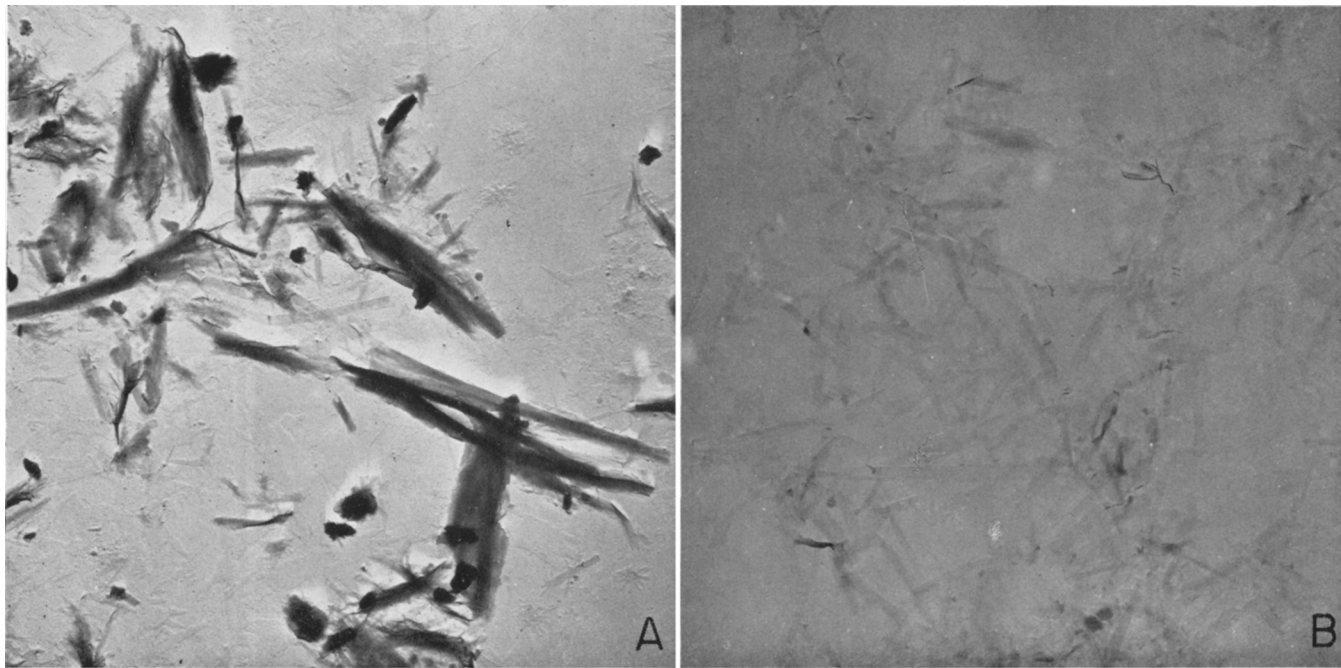


FIGURE 11.—Electron micrographs of nontronite ; shadowed with platinum at 20°. A, R_1 , magnification 7800 \times . B, R_5 , magnification 14,800 \times .

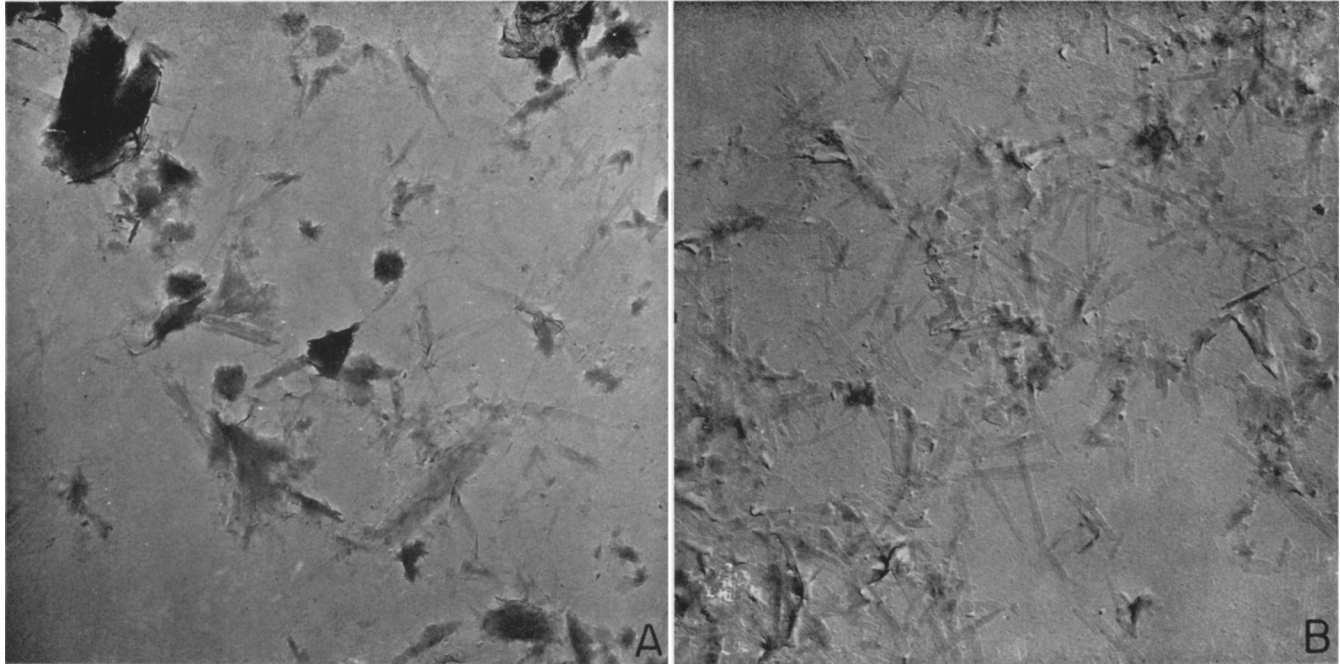


FIGURE 12.—Electron micrographs of hectorite : A, R_1 , shadowed with platinum at 20° ; magnification $11,600 \times$. B, R_3 , shadowed with platinum at 15° ; magnification $14,800 \times$.

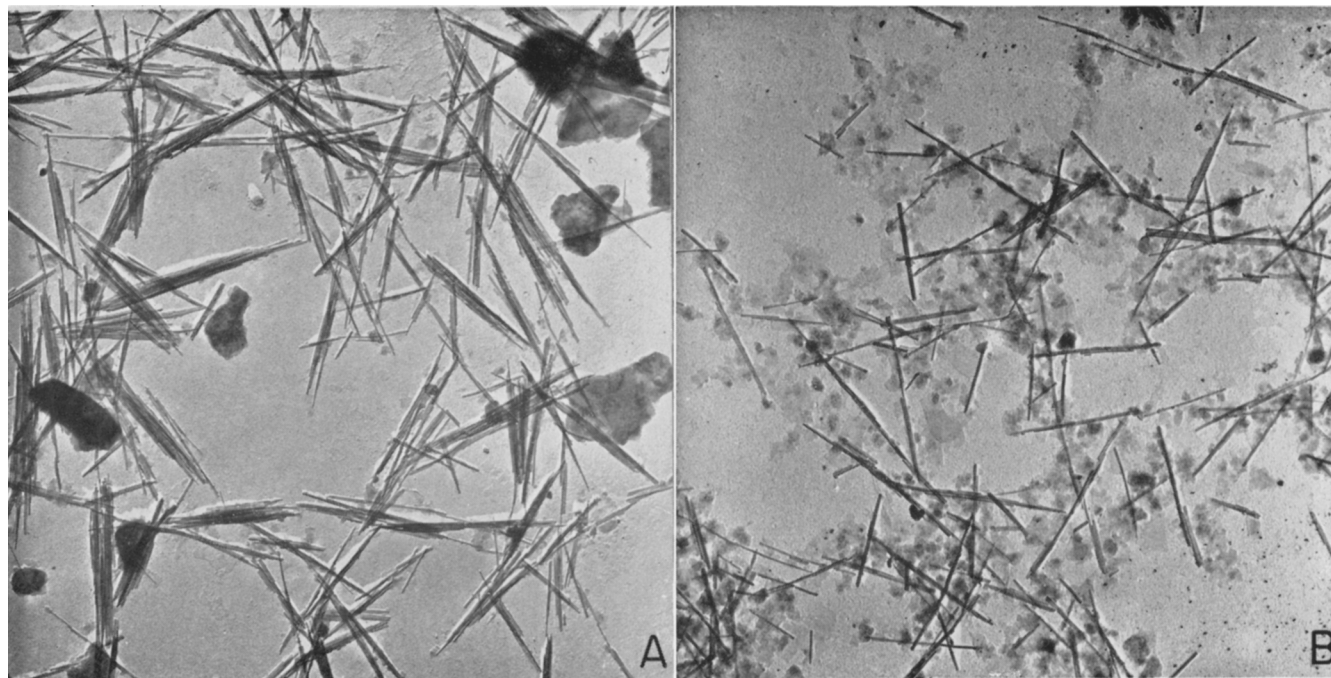


FIGURE 13.—Electron micrographs of attapulgite ; shadowed with platinum at 20°. A, R_1 , magnification 11,600 \times . B, R_5 , magnification 18,500 \times .

TABLE 7.—MAJOR DIMENSION OF CLAY MINERAL PARTICLES FROM ELECTRO-OPTICAL BIREFRINGENCE AND ELECTRON MICROSCOPY

Clay Mineral	Fraction	Major Dimension, <i>A</i>	
		Electro-optical Birefringence	Electron Microscopy
Montmorillonite	R_1	24,600	13,800
	R_2	20,600	10,800
	R_3	7600	6800
	R_4	5100	3200
	R_5	4900	2800
Illite	R_1	7400	4800
	R_2	5200	3000
	R_3	4200	2000
	R_4	3800	1200
	R_5	3600	1000
Nontronite	R_1	11,600	38,600
	R_2	11,300	17,200
	R_3	9900	14,000
	R_4	7500	10,000
	R_5	4600	6800
Hectorite	R_1	10,200–17,700	10,300
	R_2	8300–9200	6100
	R_3	7800	6100
	R_4	6700	6400
	R_5	5900	5400
Attapulgitite	R_1	18,800–32,800	15,500
	R_2	18,800–32,200	12,900
	R_3	15,800–29,000	10,800
	R_4	13,300–23,000	8800
	R_5	13,300	6600

The values for the major dimension of the clay mineral particles from electro-optical birefringence studies and from electron microscopy agree within a factor of 2 for nineteen out of the twenty-five samples, and within a factor of 3.6 for all samples. This is considered to be satisfactory agreement and shows the usefulness of the electro-optical birefringence technique in estimating the major dimensions of asymmetric particles.

2. *Thickness of particles.*—Thickness of the clay particles was determined by combining electro-optical birefringence data with either ultracentrifuge or viscosity data. The results are presented in Table 8.

The agreement between values of the thickness of clay particles from different experimental techniques is not so good as the agreement found for the major dimension of the particles. However, one can tell that the particles

TABLE 8.—THICKNESS OF CLAY MINERAL PARTICLES FROM (A) ELECTRO-OPTICAL BIREFRINGENCE AND VISCOSITY DATA, AND (B) ELECTRO-OPTICAL BIREFRINGENCE AND ULTRACENTRIFUGE DATA

Clay Mineral	Fraction	Thickness, A	
		Electro-optical Birefringence + Viscosity	Electro-optical Birefringence + Ultracentrifuge
Montmorillonite	R_1	146	64
	R_2	88	36
	R_3	28	—
	R_4	22	—
	R_5	18	—
Illite	R_1	720	164
	R_2	346	—
	R_3	172	—
	R_4	324	40
	R_5	68	—
Nontronite	R_1	64	10
	R_2	44	—
	R_3	30	—
	R_4	20	6
	R_5	14	—
Hectorite	R_1	236–410	—
	R_2	122–134	—
	R_3	42	—
	R_4	26	—
	R_5	26	—

are very thin relative to their length and, except for illite, consist of only a few layers of the fundamental clay mineral sheets. It is also of interest to note that as the major dimension decreases ($R_1 \rightarrow R_5$), the thickness also decreases. That is, there is a positive correlation between the length and thickness of the clay particles of a given type of mineral.

B. Evaluation of Methods

Any sample of clay undoubtedly has a continuously variable size and shape distribution. However, by fractionation of the clay and determination of the average length and thickness of each fraction, one can give an estimate of the distribution in terms of average dimensions for the particles in each fraction.

To obtain general concepts about the size and shape of the particles of clay materials with which one is not familiar, electron microscopy provides useful

information. The first two objections to electron microscopy presented in the introduction do not now seem valid. With improved experimental techniques, adequately clear pictures are obtainable as shown by the micrographs in this report. The second reason for the distrust of electron micrographs, namely the possibility that by the technique used in preparing the sample the original particles no longer remain, now seems unlikely since the major dimension of the particles from electron micrography is in general agreement with that obtained from electro-optical birefringence studies in all the samples studied. However, once a model for the particles is obtained from electron microscopy, one or more of the indirect methods discussed in this report is more useful in characterizing the samples.

In electron microscopy one sees only individual particles, and the problem of obtaining a representative sample is always present. In the other techniques described in this report, an average parameter for all particles is obtained from a single measurement.

The methods other than electron microscopy unfortunately must utilize calculations based on models which are mathematically simple and which may not adequately describe the particles, so that errors will be involved in absolute size measurements. However, even in these, dimensions within a factor of two are obtainable. For comparative purposes and for the characterization of clay samples by some relative average size, the indirect methods are extremely useful.

The electro-optical birefringence technique provides the most reliable data. Determination of rotational diffusion constant involves no major problems of experimental uncertainty or of theoretical assumptions. However, the calculation of a major semi-axis from this value does bring in the assumption that the particle approximates either a disk or a rod.

The ultracentrifuge technique was not very satisfactory with our instrumentation. However there is now commercially available an extremely reliable analytical ultracentrifuge which might be useful for particle size studies of clays.

The measurement of viscosity is simple but interpretation of results is not on a firm basis. However, the values obtained from the thickness of particles from the combined electro-optical birefringence and viscosity results correlate well with the qualitative ideas about this dimension obtainable from the electron micrographs.

The light-transmission method is the most difficult to interpret theoretically. It probably will be useful only as a strictly empirical tool.

C. Discussion of Individual Clay Minerals

1. *Montmorillonite*.—The platy type of structure for montmorillonite is again confirmed by the electron micrographs. The "major dimension" of the particles ranges from 2800 to 13,800 Å, a factor of five. As shown in Table 5, the particles of the largest major semi-axis also have the largest minor semi-axis.

2. *Illite*.—Illite has the smallest particles from the standpoint of lateral extent. However, illite contains by far the thickest particles, indicating a large number of stacked layers.

3. *Nontronite and hectorite*.—Nontronite and hectorite are both lathlike in the electron micrographs. From the viscosity data they seem very asymmetric and may contain only a few layers of the fundamental structural sheets.

4. *Attapulgitite*.—The structure of attapulgitite is unequivocally rod-shaped from the electron micrographs. The average lengths of the rods in the various fractions range from 6600 to 15,500 Å. There does not seem to be much change in diameter from sample R_1 to R_5 .

9. SUMMARY AND CONCLUSIONS

The particle size and shape of montmorillonite, illite, nontronite, hectorite and attapulgitite were studied by five techniques—electro-optical birefringence, ultracentrifugation, viscosity, light transmission and electron microscopy. The total range of the maximum dimension of the particles was from 1000 to 38,600 Å.

It is concluded that for a preliminary survey of the size and shape of clay mineral particles, electron microscopy is most useful. However, once a model for the particles is obtained, a combination of electro-optical birefringence and viscosity data provides a much more convenient method for obtaining the major dimension and the thickness of the clay particles.

REFERENCES

- Alexander, A. E. and Johnson, P. (1949) *Colloid Science*, v. 1, Oxford University Press, New York, 554 pp.
- Bender, M. (1952) The use of light scattering for determining particle size and molecular weight and shape : *J. Chem. Educ.*, v. 29, pp. 15–23.
- Benoit, H. (1951) The Kerr effect demonstrated by dilute solutions of rigid macromolecules : *Ann. Phys.*, v. 6, pp. 561–609.
- Doty, P. and Steiner, R. F. (1950) Light scattering and spectrophotometry of colloidal solutions : *J. Chem. Phys.*, v. 18, pp. 1211–1220.
- Kahn, A. and Lewis, D. R. (1954) The size of sodium montmorillonite particles in suspension from electro-optical birefringence studies : *J. Phys. Chem.*, v. 58, pp. 801–804.
- Kelley, O. J. and Shaw, B. T. (1942) Studies of clay particles with the electron microscope : III. Hydrodynamic considerations in relation to shape of particles : *Soil Sci. Soc. Amer. Proc.*, v. 1, pp. 58–68.
- Mark, H. and Tobolsky, A. V. (1950) *Physical Chemistry of High Polymeric Systems* : Interscience Publishers Inc., New York, 506 pp.
- Marshall, C. E. (1949) *The Colloid Chemistry of the Silicate Minerals* : Academic Press, Inc., New York, 162 pp.
- Svedberg, T. and Pederson, K. O. (1940) *The Ultracentrifuge* : Oxford University Press, New York, 478 pp.
- van Olphen, H. (1950) Stabilization of montmorillonite sols by chemical treatment : *Rec. de Trav. Pays-Bas*, v. 69, pp. 1313–1322.
- van Olphen, H. (1951) Chemical treatment of drilling fluids : Thesis, Delft.